

Authors are encouraged to submit new papers to INFORMS journals by means of a style file template, which includes the journal title. However, use of a template does not certify that the paper has been accepted for publication in the named journal. INFORMS journal templates are for the exclusive purpose of submitting to an INFORMS journal and should not be used to distribute the papers in print or online or to submit the papers to another publication.

# Bayesian Structural Inference for Dynamic Crowdsourcing Contests

Jussi Keppo

NUS Business School and Institute of Operations Research and Analytics  
National University of Singapore, Singapore  
keppo@nus.edu.sg

Linsheng Zhuang

Institute of Operations Research and Analytics  
National University of Singapore, Singapore  
linsheng.z@u.nus.edu

...

*Key words:* Digital Economy, Data Protection Regulation, Innovation Contest

## 1. Introduction

- Kaggle<sup>1</sup> ...
- Meta-kaggle dataset [Risdal and Bozsolik \(2022\)](#).

### 1.1. Related Literature

This paper focuses on the two players innovation contest with a continuous time where the players' relative position is public information throughout the game. This is closely related to tug-of-war contest, which, to our knowledge, was first formally given by [Harris and Vickers \(1987\)](#) as a one-dimensional simplification of the multi-stage R&D race. The output processes are model by Brownian motions drifted with effort inputs, which is followed by [Budd et al. \(1993\)](#) who model the state of a dynamic competition of two innovative duopoly firms by a Brownian motion drifted by the effort gap, and solve the equilibrium approximately. Furthermore, [Moscarini and Smith \(2011\)](#) model the tug-of-war state as the gap of the two outputs directly, and draw an analytical equilibrium of the pure strategies.

<sup>1</sup> <https://www.kaggle.com>

...

Information disclosure in contest - [Bimpikis et al. \(2019\)](#).

...

Closest paper - [Ryvkin \(2022\)](#).

...

## 2. The Model

Two players,  $i$  and  $j$ , compete for a prize  $\theta > 0$  in a contest. Winner gets the prize and loser gets nothing. The contest starts at time zero. At every time  $t \geq 0$ , the representative player  $i$  chooses an effort level  $q_{i,t}$  and burdens a quadratic cost  $C_i(q_{i,t}) = c_i q_{i,t}^2 / 2$ , with a lower  $c_i$  corresponding to higher ability. Denoted by  $y_t$  the *output gap* of player  $i$  and  $j$  at time  $t$ , driven by

$$dy_t = (q_{i,t} - q_{j,t})dt + \sigma dW_t \quad (1)$$

where  $W_t$  is a Brownian motion and  $\sigma > 0$  measures the innovation risk.

The contest is equipped with a submission system that allows participants to upload their algorithms at any time and receive immediate feedback. For simplicity, we further assume that agents submit their intermediate results whenever they make progress. This setup enables the contest organizers to monitor all players' progress  $x_{i,t}$  and  $x_{j,t}$  in real time. Moreover, the true output level, evaluated by the system, is only known by the game designer but not the two players. At any time  $t > 0$ , the contest designer emits a *public* signal of the real output gap  $y_t$ . The signal is ambiguous and the game holder controls the ambiguity. The dynamic of signal is

$$dZ_t = y_t dt + \frac{dB_t}{\sqrt{\lambda}} \quad (2)$$

where  $B_t$  is standard Brownian motion independent with  $(W_{i,t})$  and  $(W_{j,t})$ , and the parameter  $\lambda$  is set by the game holder to control the precision of signal. The larger the  $\lambda$ , the more accurate the signal would be.

The information set of both players at time  $t \geq 0$  is  $I_t \equiv \{Z_s : 0 \leq s \leq t\}$ . Player  $i$  estimates the unknown output gap  $y_t$  based on the information set  $I_t$ . Let  $\tilde{y}_t \equiv E(y_t | I_t)$  be the estimated output gap and  $S_t \equiv E[(\tilde{y}_t - y_t)^2 | I_t]$  be the estimation variance. According to Chapter 1.2 of [Bensoussan \(1992\)](#), *Kalman-Bucy filter* gives the dynamics of  $\tilde{y}_t$  and  $S_t$ ,

$$d\tilde{y}_t = (q_{i,t} - q_{j,t})dt + \lambda S_t (dZ_t - \tilde{y}_t dt) \quad (3)$$

$$\frac{dS_t}{dt} = \sigma^2 - \lambda S_t^2 \quad (4)$$

Hence, the conditional distribution  $y_t|I_t \sim \mathcal{N}(\tilde{y}_t, S_t|I_t)$  is fully captured by the mean  $\tilde{y}_t$  and variance  $S_t$ . If  $\lambda = 0$ , we have  $S_t = S_0 + \sigma^2 t$ , i.e., the estimation variance is increasing in time linearly. If  $\lambda > 0$ , the solution of (17) is

$$S_t = \begin{cases} \bar{S} \cdot \tanh \left\{ t \cdot \sigma \sqrt{\lambda} + \tanh^{-1} (S_0/\bar{S}) \right\} & \text{if } S_0 < \bar{S} \\ \bar{S} & \text{if } S_0 = \bar{S} \\ \bar{S} \cdot \coth \left\{ t \cdot \sigma \sqrt{\lambda} + \coth^{-1} (S_0/\bar{S}) \right\} & \text{if } S_0 > \bar{S} \end{cases} \quad (5)$$

Specifically,  $\bar{S} = \sigma/\sqrt{\lambda}$  when  $\lambda > 0$  and  $\bar{S} = \infty$  when  $\lambda = 0$ . Please refer to Appendix C.1 for the derivations. Figure 1 shows the evolution of  $S_t$  in time: estimation variance  $S_t$  converges to *steady state*  $\bar{S}$  as time goes by regardless of the starting estimation variance. For simplicity, we henceforth assume that  $S_0 = \bar{S}$ , hence  $S_t \equiv \bar{S}$ .



**Figure 1** The evolution of  $S_t$  in time  $t$ , given that  $\lambda = 1$  and  $\sigma = 1$ .

Following Ryvkin (2022), let's consider a dynamic contest with a fixed deadline. Suppose the contest is terminated when time  $t = T > 0$ . Since the steady state estimation variance  $\bar{S}$  is fixed as displayed above, the state of the game is fully characterized by a tuple  $(\tilde{y}_t, t)$ . At any time  $0 \leq t < T$ , player  $i$  optimizes her effort level  $q_{i,\tau}$  in the remaining contest period  $\tau \in [t, T)$  according to the following optimization problem,

$$V^i(\tilde{y}_t, t; q_{j,t}, \Theta_i) = \max_{\{q_{i,\tau}\}_{\tau=t}^T} \mathbb{E} \left( \theta \cdot 1_{\tilde{y}_T > 0} - \int_t^T C_i(q_{i,\tau}) d\tau \middle| I_t \right) \quad (6)$$

where  $\Theta_i \equiv \{\theta, \lambda, \sigma, c_i\}$ , subject to constraints (16), (17) and  $q_{i,\tau} \geq 0$  for all  $\tau \in [t, T)$ . The optimization problem for player  $j$  is just symmetric to that of player  $i$  as  $V^j(\tilde{y}_t, t) = V^i(-\tilde{y}_t, t)$ . The corresponding Hamilton-Jacobi-Bellman (HJB) equation for player  $i$  is

$$0 = \max_{q_{i,t} \geq 0} \left[ -\frac{c_i q_i^2}{2} + V_y^i \cdot (q_{i,t} - q_{j,t}) + V_t^i + \frac{V_{yy}^i}{2} \lambda \bar{S}^2 \right]$$

By definition, we have  $\lambda \bar{S}^2 = \sigma^2$ . Under the assumption of inner solution, we plug into the first order conditions  $q_{i,t} = V_y^i / c_i$  and  $q_{j,t} = -V_y^j / c_j$ , we have the system of equations

$$\begin{aligned} \frac{1}{2c_i}(V_y^i)^2 + \frac{1}{c_j}V_y^i V_y^j + V_t^i + V_{yy}^i \frac{\sigma^2}{2} &= 0 \\ \frac{1}{2c_j}(V_y^j)^2 + \frac{1}{c_i}V_y^j V_y^i + V_t^j + V_{yy}^j \frac{\sigma^2}{2} &= 0 \end{aligned}$$

subject to boundary conditions  $V^i(-\infty, t) = 0$ ,  $V^i(+\infty, t) = \theta$ ,  $V^j(-\infty, t) = \theta$ ,  $V^j(+\infty, t) = 0$ ,  $V^i(\tilde{y}_T, T) = \theta \cdot 1_{\tilde{y}_T > 0}$  and  $V^j(\tilde{y}_T, T) = \theta \cdot 1_{\tilde{y}_T < 0}$ .

The Nash equilibrium is summarized in the following lemma. We include a simplified version of the proof in the appendix:

LEMMA 1 (**Ryvkin 2022**). *In the Markov perfect equilibrium, the players' efforts in state  $m_{i(j)}(\tilde{y}_t, t) : \mathbb{R} \times [0, T) \rightarrow \mathbb{R}_+$  are given by*

$$m_{i(j)}(\tilde{y}_t, t) = \frac{e^{-z^2/2}}{\sqrt{2\pi\sigma^2(T-t)}} \cdot \frac{\sigma^2}{2} [\gamma(\rho_i) + \gamma(\rho_j)] [1 - \rho(z)^2] [1 \pm \rho(z)] \quad (7)$$

where  $z = \tilde{y}_t / (\sigma\sqrt{T-t})$ ,  $\rho(z) = \gamma^{-1}(\Phi(z) [\gamma(\rho_i) + \gamma(\rho_j)] - \gamma(\rho_j))$  and

$$\gamma(u) = \frac{u}{1-u^2} + \frac{1}{2} \ln \frac{1+u}{1-u}, \quad u \in (-1, 1)$$

$$\rho_i = \frac{e^{w_i} + e^{-w_j} - 2}{e^{w_i} - e^{-w_j}}, \quad \rho_j = \frac{e^{w_j} + e^{-w_i} - 2}{e^{w_j} - e^{-w_i}}, \quad w_{i(j)} = \frac{\theta}{\sigma^2 c_{i(j)}}.$$

The variables  $w_{i(j)}$  represent the abilities of two players, while  $\rho_{i(j)}$  normalizes  $w_{i(j)}$  into the interval  $(-1, 1)$ . It is not hard to see that  $\gamma(\cdot)$  is strictly increasing on  $(-1, 1)$ , ranging from  $-\infty$  to  $+\infty$ . Moreover, the equilibrium effort  $m_{i(j)}$  can be represented to the product of  $\phi(y; 0, \sigma^2(T-t))$ , the probability density of normal distribution with mean zero and variance  $\sigma^2(T-t)$  at the state  $y$  and an amplitude factor that only depends on the composite variable  $z$ .

To Do: Contest Design Rules

PROPOSITION 1. ...

### 3. Estimation Framework

In this section, we describe the estimation procedure. We first outline the data generation process, establishing the connection between the empirical data and the theoretical model discussed previously. Then, we introduce a structural estimation method using Bayesian framework.

### 3.1. Data-Generating Process

For each Kaggle contest, the observable data from the Meta-Kaggle dataset can be categorized into three main components:

The first component consists of essential contest details, including the contest duration, prize structure, information disclosure policy, and other governing rules. Contrary to the assumptions of our model, a typical contest usually involves multiple teams rather than just two. In Section 5, we focus on the two strongest participants in each contest for analysis; further discussion on this choice is provided in Section B.1. Furthermore, many contests adopt complex prize structures, offering multiple awards rather than following a winner-takes-all format. In Section 5, we begin by selecting contests that offer a single prize awarded in USD. Extensions to more general prize structures are presented in Section B.1.

The second component captures the submission events of each player  $i$  to the system, denoted by the sequence  $\{\hat{t}_k^i\}_{k=1}^{N_i}$ . Here,  $N_i$  represents for the total number of submissions by player  $i$ , and  $t$  represents for the time of each submission. We understand the submission events of player  $i$  and  $j$  as two conditional independent inhomogeneous Poisson processes, driven by the intensity functions  $\tau_i(t)$  and  $\tau_j(t)$ .<sup>2</sup> Then, during any time interval  $\mathcal{S}$  of the contest duration  $\mathcal{T}$ , the Poisson arrival rate of submissions of the representative player  $i$  is given by  $\int_{s \in \mathcal{S}} \tau_i(s) ds$ . We assume the submission intensity  $\tau_i(t)$  is proportional to the effort level  $m_i(\tilde{y}_t, t)$ . More specifically,

$$\tau_i(t) = r \cdot m_i(\tilde{y}_t, t) \quad (8)$$

where  $r > 0$  is the ratio of submission intensity and effort level. The contest players are aware of this ratio, but the contest designer must infer it from the data.

The third component of the contest data is the *public* and *private* leaderboard that records the real-time rankings and scores of each participant, denoted by  $\hat{x}_t^{i(j)}$  and  $x_t^{i(j)}$ . In Kaggle competitions, most organizers deliberately disclose only a subset of the full dataset to participants to mitigate the risk of overfitting. The proportion of the released data is generally known to all participants. The public leaderboard is updated upon each submission, using only the released portion of the dataset; as a result, the signals it provides are inherently noisy. In addition to the public leaderboard, most competitions hosted on Kaggle also maintain a private leaderboard, where organizers evaluate the true predictive performance of participants' models using the full dataset. The true output gap  $y_t := x_t^i - x_t^j$  is generated according to equation (1). It is observable only by the game designer during the contest and becomes available from the Meta-Kaggle dataset after the contest

<sup>2</sup> That is, given the intensity functions  $\tau_i(t)$  and  $\tau_j(t)$ , the submission events  $\{\hat{t}_k^i\}_{k=1}^{N_i}$  and  $\{\hat{t}_k^j\}_{k=1}^{N_j}$  are mutually independent.

concludes. Furthermore, we interpret the difference in scores between  $i$  and  $j$  displayed on the public leaderboard as the signal  $Z_t$  defined in (15), released by the contest organizer. Specifically, let's denote  $\hat{y}_t = \hat{x}_t^i - \hat{x}_t^j$  the gap between displayed scores, and interpret it as the signal intentionally released by the contest organizer:

$$dZ_t = \hat{y}_t dt \quad (9)$$

Combining (15) with (1), the observed real-time gap  $\hat{y}_t$  on leaderboard evolves as

$$\hat{y}_t = y_t + \frac{1}{\sqrt{\lambda}} \frac{dB_t}{dt} = \int_0^t [m_i(\tilde{y}_t, s) - m_j(\tilde{y}_t, s)] ds + \sigma W_t + \frac{\xi_t}{\sqrt{\lambda}} \quad (10)$$

where the term  $\sigma W_t$  captures the accumulated innovation shock,  $\lambda$  governs the signal precision and  $\xi_t$  is a white noise with  $\mathbb{E}(\xi_t \xi_s) = \delta(t - s)$ . In practise, we approximately assume that  $\xi_t \approx (B_{t+\Delta} - B_t)/\Delta$  where  $\Delta$  is a small time interval.

Beyond the uncertainty introduced by partial data disclosure, a second source of signal noise arises from the timing of leaderboard updates: rankings are refreshed only after model submissions, leaving the leaderboard uninformative during periods without new submissions. It should be noted that such lag would significantly bias our model estimates only if participants strategically timed their submissions. Although such strategic behaviour is theoretically possible, we abstract from it in this study. We assume that each submission follows a period of substantive effort, allowing the leaderboard rankings to broadly reflect the relative performance of algorithms based on the publicly available data.

It is important to recognize that the generation of  $y_t$  and  $\hat{y}_t$  is inherently tied to the players' strategic interactions, as it depends on their estimates of the underlying state,  $\tilde{y}_t$ . In turn,  $\tilde{y}_t$  evolves dynamically based on  $\hat{y}_t$ , since players continually update their beliefs in response to observed data. As a result, the generation of  $y_t$ ,  $\hat{y}_t$  and  $\tilde{y}_t$  proceeds jointly. By equations (16) and (9), the estimated gap  $\tilde{y}_t$  as perceived by the two players, is determined by the following stochastic differential equation:

$$d\tilde{y}_t = [m_i(\tilde{y}_t, t) - m_j(\tilde{y}_t, t)] dt + \sqrt{\lambda} \sigma (\hat{y}_t - \tilde{y}_t) dt \quad (11)$$

with initial condition  $\tilde{y}_0 = \mu_0$ , where  $\mu_0$  can be interpreted as the prior mean of the initial true state  $y_0$ .

We denote the set of unknown parameters by  $\Theta := \{c_i, c_j, r, \sigma, \lambda, \mu_0\}$ . Once  $\Theta$  is specified, the data-generating processes for  $(y_t)$ ,  $(\hat{y}_t)$ , and  $(\tilde{y}_t)$  are fully defined by equations (1), (10), and (11), although their realized trajectories remain stochastic.

### 3.2. Bayesian Estimation Framework

Our objective is to develop a Bayesian framework for inferring the unknown parameter set  $\Theta := \{c_i, c_j, r, \sigma, \lambda, \mu_0\}$  using the data introduced above.

First of all, we assume that time is discretized into uniform intervals of length  $\Delta$ . By definition, the likelihood function corresponding to the submission times of player  $i$ ,  $\{t_k^i\}_{k=1}^{N_i}$ , is given as follows (a symmetric formulation applies to player  $j$ ):

$$p\left(\{t_k^i\}_{k=1}^{N_i} | \tau_i, \Theta\right) = \exp\left\{-\int_{s \in \mathcal{T}} \tau_i(s) ds\right\} \prod_{k=1}^{N_i} \tau_i(t_k^i) \quad (12)$$

where  $\tau_i$  is defined in (8) with the tuning parameter  $r$  exogenously specified. Since time is discretized, the integrals on the left-hand side can be approximated by finite sums.

Next, suppose the public leaderboard gaps  $\hat{y}_t$  is sampled at time points  $(t_1, t_2, \dots, t_N)$ , yielding observations  $\{\hat{y}_{t_k}\}_{k=1}^N$ . Let  $t_0 = 0$  and suppose the initial gap satisfies  $y_0 = 0$ . Then, according to the assumed data-generating process of  $\hat{y}_t$  in (10), the corresponding likelihood function is

$$p\left(\{\hat{y}_{t_k}\}_{k=1}^N | \{\tilde{t}_k^{(j)}\}_{k=1}^{N_i(j)}, m_i, m_j, \Theta\right) = \phi\left(\{\hat{y}_{t_k}\}_{k=1}^N | \{\mu_k\}_{k=1}^N, \Sigma_y + \frac{I_N}{\Delta\lambda}\right) \quad (13)$$

where  $\mu_k = \int_0^{t_k} m_i(\tilde{y}_s, s) - m_j(\tilde{y}_s, s) ds$  and  $\Sigma_y(i, j) = \sigma^2 \min(t_i, t_j)$ . Moreover, let  $N = N_i + N_j$ , indicating that the public leaderboard is updated once a new submission occurs.

It's worthwhile noting that, although the trajectory of private leaderboard  $y_t$  is available ex post from the Meta-Kaggle dataset, we deliberately exclude it from the likelihood function. In our framework, agents form beliefs about  $y_t$  based solely on  $\hat{y}_t$ , and their actions are driven by these beliefs. Conditioning on the realized values of  $y_t$  in estimation would effectively bypass the agent's informational constraints and undermine the role of  $\lambda$  in shaping belief formation. More importantly, it would prevent us from evaluating whether the proposed model—when given only the information actually available to agents—can recover the true data-generating process. Treating  $y_t$  as latent therefore preserves the integrity of the causal structure and enables meaningful model validation after estimation.

To evaluate the likelihood functions (12) and (13), we must first compute the equilibrium trajectories of both the perceived output gap ( $\tilde{y}_t$ ) and the effort levels  $(m_i(\tilde{y}_t, t), m_j(\tilde{y}_t, t))$ , as implied by equations (7) and (11). Importantly, the construction of  $\tilde{y}$  and the effort functions  $m_i$  and  $m_j$  depends on the underlying (unobserved) parameters  $c_i, c_j, \sigma$  and  $\lambda$ , which are themselves subject to estimation. We denote these underlying parameters collectively as  $\mathcal{P}$ .

Once these parameters are specified, the equilibrium paths of the perceived output gap ( $\tilde{y}_t$ ) and the corresponding effort levels  $(m_i(\tilde{y}_t, t), m_j(\tilde{y}_t, t))$  can be deterministically computed. However, evaluating  $m_{i(j)}(\tilde{y}_t, t)$  via equation (7) requires numerically approximating the inverse function  $\gamma^{-1}$ ,

which poses challenges for the use of gradient-based Markov Chain Monte Carlo (MCMC) sampling methods, such as Hamiltonian Monte Carlo (HMC, Neal 1996, Neal 2011, Betancourt 2017) and the No-U-Turn Sampler (NUTS, Hoffman and Gelman 2014). Hence, we approximate this inverse function with an analytical form:

$$\gamma^{-1}(x) \approx \frac{2}{\pi} \arctan(a \cdot x) \quad (14)$$

where  $a$  is around 0.947 by minimizing the 1-norm of the difference between the numerical inverse of  $\gamma(\cdot)$  and the approximation  $\frac{2}{\pi} \arctan(ax)$ .<sup>3</sup> Figure 4 compares the equilibrium effort function  $m_i(\tilde{y}_t, t)$  derived from the approximate analytical form of  $\gamma^{-1}$  in equation (14) with that obtained from the numerically accurate solution. As illustrated, the approximation closely replicates the true function.

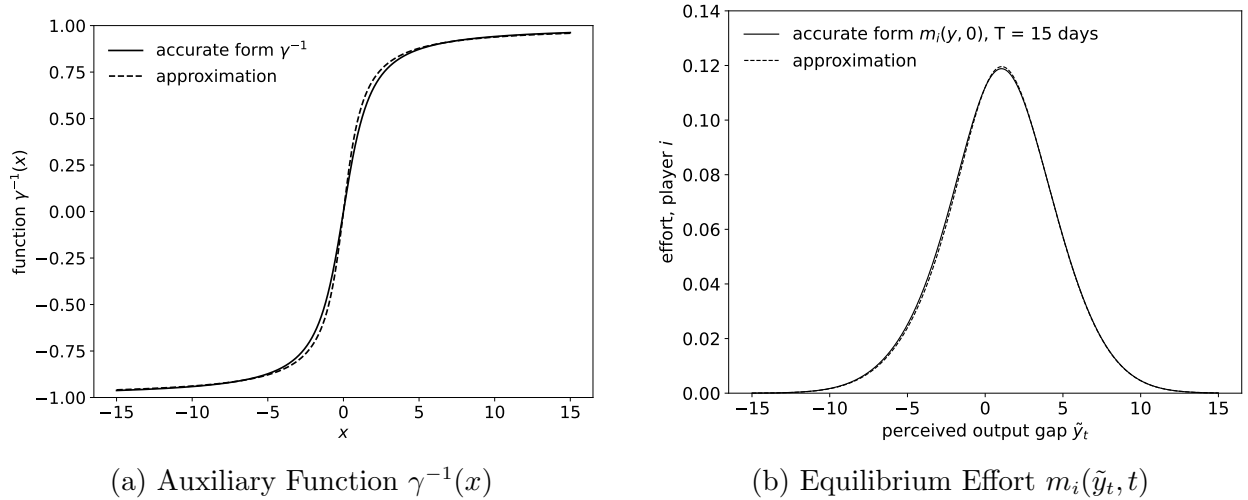


**Figure 2** Comparison of the Accurate and Approximate Forms ( $\theta = 1$ ,  $c_i = c_j = 1$ ,  $\sigma = 1$ ,  $\Delta = 1/24$ )

In our Bayesian framework, we specify truncated normal distributions with large variances as priors for the unknown parameters  $\Theta$ .<sup>4</sup> This choice is intended to make the priors as uninformative as possible, thereby minimizing their influence on the posterior distribution. By allowing the parameters to vary broadly within reasonable bounds, these weakly informative priors let the data play a dominant role in shaping the inference, while still ensuring mathematical well-posedness and numerical stability.

The following lemma establishes the identifiability of the model parameters.

**LEMMA 2.** *The contest parameters  $c_i$ ,  $c_j$ ,  $r$ ,  $\sigma$ ,  $\lambda$  and  $\mu_0$  are jointly identifiable.*

<sup>3</sup> Under infinity norm, the parameter  $a = 0.856$ ; under 2-norm, the parameter  $a = 0.895$ .

<sup>4</sup> Specifically, each of these parameters is assigned a truncated normal prior with mean 1, variance 5, and support on either the interval  $[0.5, 5]$ ,  $[0.5, 10]$  or  $[1e-6, 10]$ , depending on the numerical stability considerations.



## 4. Synthetic Experiments

Before applying our estimation procedure to real-world contest data, we evaluate its potential on synthetically generated data. The use of synthetic data serves not only to validate the effectiveness of Bayesian inference, but also to enhance our understanding of the underlying data-generating process, which is summarized in Algorithm 1.

---

### Algorithm 1 Synthetic Data Simulation

---

**Input:**  $\Delta, T, c_i, c_j, \sigma, \lambda, r, \tau^*, y_0, \mu_0$

Sample  $\{s_k^{i(j)}\}_{k=1}^{N_{i(j)}}$  from Poisson process  $(\tau^*)$  on  $[0, T]$

Sample  $\{u_k^{i(j)}\}_{k=1}^{N_{i(j)}}$  from uniform distribution on  $[0, 1]$

Sample series of Brownian motions  $(W_t)$  and  $(B_t)$

Initialize  $\ell^{i(j)} = 0, \hat{y}_0 = 0, \tilde{y}_t = \mu_0$

**for**  $t = 0$  to  $T$  **do**

$m_{i(j)}(\tilde{y}_t, t) \leftarrow (7), \tau^{i(j)}(t) \leftarrow (8)$  {Use  $\theta, c_{i(j)}, \sigma, r, T$ }

$y_{t+\Delta} \leftarrow (1); \tilde{y}_{t+\Delta} \leftarrow (11)$  {Use  $\sigma, \lambda, \Delta, W_{t+\Delta}, y_0$ }

**for**  $s_k^{i(j)} \in [t, t + \Delta]$  **do**

**if**  $u_k^{i(j)} < \tau_{i(j)}(s_k^{i(j)})/\tau_{i(j)}^*$  **then**

$\hat{t}_\ell^{i(j)} \leftarrow s_k^{i(j)}; \ell^{i(j)} \leftarrow \ell^{i(j)} + 1$  {Accept the submission event}

$\hat{y}_{t+\Delta} \leftarrow (10)$  {Use  $\sigma, \lambda, B_{t+\Delta}$ }

**end if**

**end for**

**end for**

**Output:**  $(y_t), (\tilde{y}_t), (m_{i(j)}(\tilde{y}_t, t)), \{\hat{t}_k^{i(j)}\}_{k=1}^{N_{i(j)}}, (\hat{y}_{t_k})_{k=1}^{N_i+N_j}$

---

A central challenge in generating synthetic data lies in dynamically constructing a point process that conforms to an inhomogeneous Poisson process. We first generate candidate submission events according to a homogeneous Poisson process over the whole contest duration, using a fixed high intensity  $\tau^* \geq \sup_t \tau_{i(j)}(t)$ . Then, we apply the classical thinning procedure (Lewis and Shedler 1979) to determine whether each candidate event is accepted or not.

As a concrete example, we consider an artificial contest that spans a three-month period, from January 1 to April 1, 2025. The contest involves two participants,  $i$  and  $j$ , who differ slightly in their effort costs. Specifically, the unit costs of effort are set to  $c_i = 1.2$  and  $c_j = 1.5$ , respectively. The innovation risk of the contest is assumed to be  $\sigma = 2.0$ , and the precision of the signal is set to  $\lambda = 1.0$ . The prize value  $\theta$  is normalized to one. Additionally, we assume the ratio between submission intensity and effort is given by  $r = 15$ . Under this specification, we simulate the trajectory of the true

output gap ( $y_t$ ), the submission times  $\{t_k^i\}_{k=1}^{N_i}$  and  $\{t_k^j\}_{k=1}^{N_j}$  for both players, and the corresponding updates to the public leaderboard  $(\hat{y}_{t_k})_{k=1}^{N_i+N_j}$ . We also compute the perceived output gap ( $\tilde{y}_t$ ) over time, as well as the equilibrium effort levels  $(m_i(\tilde{y}_t, t))$  and  $(m_j(\tilde{y}_t, t))$ .

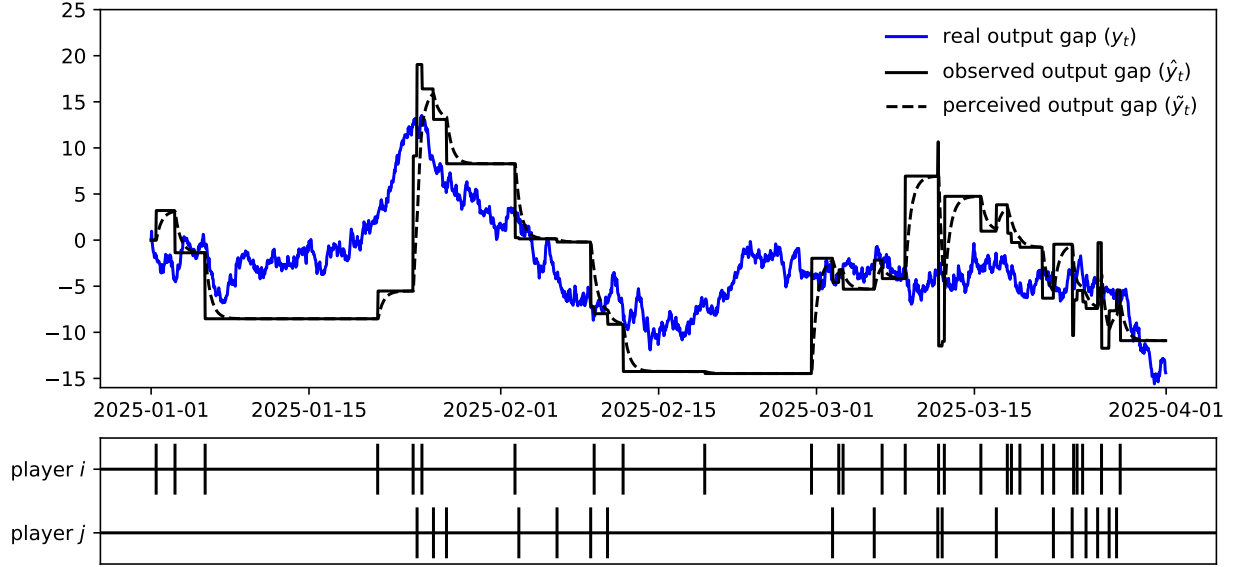


**Figure 3 Synthetic Contest Data of Two Players from 2025-01-01 to 2025-04-01**

( $\theta = 1.0$ ,  $c_i = 1.2$ ,  $c_j = 1.5$ ,  $\sigma = 2.0$ ,  $\lambda = 1.0$ ,  $r = 15$ )

Figure 3 shows a realization of the virtual contest described above. The blue line in Figure 3 represents the underline true output gap  $y_t$ , which can be interpreted as a *private* leaderboard visible only to the contest designer, who has exclusive access to the full dataset. Its drift is determined by the cumulative effort gap between the two players, while its volatility is governed by the contest's innovation risk parameter  $\sigma$ . The solid black line depicts the corresponding *public* leaderboard  $\hat{y}_t$ , which is updated whenever a submission is made by either player  $i$  or  $j$ , as indicated by the short vertical ticks. Intuitively, the more information is disclosed, the more closely the public leaderboard  $\hat{y}_{t_k}$  approximates the true state  $y_{t_k}$ ; the level of signal noise is controlled by the precision parameter  $\lambda$ . The dashed black line shows the players' perceived output gap  $\tilde{y}_t$ , as inferred from the public leaderboard and defined in equation (11). Submission times  $\hat{t}_k^i$  and  $\hat{t}_k^j$ , marked by the short vertical ticks, are driven by each player's effort level and are modelled as realizations of an inhomogeneous Poisson process. There are 28 submissions from player  $i$  and 18 submissions from player  $j$ .

One might observe that, between two submissions  $\hat{t}_k$  and  $\hat{t}_{k+1}$ , the estimate variance of the two players  $S_t$  should increase over time rather than remain constant as we have assumed. However, under our modelling assumption where no submission implies low effort, a Bayesian player would

infer that inactivity signals low intensity, thereby narrowing the estimation variance. For analytical tractability and to leverage the steady-state equilibrium formulation (7), we abstract from modelling time-varying uncertainty.

**Table 1** Bayesian Estimates from Synthetic Data

Parameters (true val.)	$c_i$	$c_j$	$r$	$\sigma$	$\lambda$	$\mu_0$
	1.2	1.5	15.0	2.0	1.0	0.0
Posterior Mean	1.078	1.711	14.645	2.777	1.103	-0.010
Posterior Std.	0.382	0.661	3.986	0.503	0.303	2.026
RMSE	0.401	0.694	4.002	0.925	0.320	2.026
95% Interval	[0.55, 1.99]	[0.77, 3.30]	[7.8, 23.0]	[1.94, 3.93]	[0.61, 1.79]	[-3.97, 4.00]

Note:  $\text{MSE}(\hat{\theta}) = \mathbb{E}(\hat{\theta} - \theta)^2 = [\mathbb{E}(\hat{\theta}) - \theta]^2 + \text{Var}(\hat{\theta})$  by the bias–variance decomposition. RMSE is then calculate by the squared root of MSE.

Table 1 presents the Bayesian inference results based on the synthetic data that we display in Figure 3. Due to the limited data from the short contest duration, the posterior distribution of some parameters (such as  $\sigma$  in this example) remains relatively far from the true value. Nevertheless, given the limited sample size, the performance of Bayesian estimation is satisfactory. For most parameters (specifically  $c_i$ ,  $c_j$ ,  $r$ ,  $\lambda$  and  $\mu_0$ ), the posterior means lie reasonably close to their true values.

We next examine whether Bayesian estimation improves with increasing data quantity.

#### 4.1. Asymptotic Properties

With the synthetic contest data in place, it is important to ensure that our Bayesian framework is statistically coherent and implemented correctly. To this end, we numerically examine the asymptotic behaviour of the posterior distribution under two scenarios: *i*) repeating the experiment multiple times under a fixed data-generating process, and *ii*) observing a single contest over an long time horizon. As the amount of data increases, posterior consistency ensures that the Bayesian posterior concentrates around the true parameter values (Vaart 1998, Ghosal et al. 2000, Pokern et al. 2013, Ramamoorthi et al. 2015). While our analysis is simulation-based rather than theoretical, it provides evidence that the proposed likelihood formulation and inference procedure behave as expected in large-sample regimes.

**4.1.1. Replications.** To begin, we investigate the asymptotic behavior of the posterior distribution when multiple independent realizations of the contest are observed. Multiple contests are independently simulated under identical parameters, with their data pooled to form a larger sample for Bayesian inference. This setting corresponds to a replicated experimental design and

allows us to assess whether Bayesian inference consistently recovers the true parameters as the number of observed contests increases.

The experimental results are presented in Table 2. We replicate the contest simulation with 5, 10, and 20 independent instances. As the sample size increases, the RMSE of all parameters decreases, indicating that the posterior distributions converge more closely to the true parameter values.

**Table 2 Bayesian Estimates from Pooled Synthetic Data**

Parameters	$c_i$	$c_j$	$r$	$\sigma$	$\lambda$	$\mu_0$
(true val.)	1.2	1.5	15.0	2.0	1.0	0.0
<b>Pool of 5 Contests</b>						
Posterior Mean	1.215	1.647		1.969	1.079	
Posterior Std.	0.120	0.178		0.143	0.130	
RMSE	0.121	0.231		0.146	0.152	
<b>Pool of 10 Contests</b>						
Posterior Mean	1.255	1.690		1.911	1.053	
Posterior Std.	0.090	0.129		0.096	0.090	
RMSE	0.105	0.230		0.131	0.105	
<b>Pool of 20 Contests</b>						
Posterior Mean	1.206	1.639		1.981	0.990	
Posterior Std.	0.059	0.090		0.069	0.059	
RMSE	0.060	0.165		0.071	0.060	

Note:  $MSE(\hat{\theta}) = \mathbb{E}(\hat{\theta} - \theta)^2 = [\mathbb{E}(\hat{\theta}) - \theta]^2 + Var(\hat{\theta})$  by the bias–variance decomposition. RMSE is then calculate by the squared root of MSE.

**Table 3 Bayesian Estimates from Long Term Synthetic Data**

Parameters	$c_i$	$c_j$	$r$	$\sigma$	$\lambda$	$\mu_0$
<b>Contest of 6 Months</b>						
True Value	0.6	0.75	15.0	2.0	1.0	0.0
Posterior Mean	0.840	0.835	.	1.944	1.142	
Posterior Std.	0.138	0.152	.	0.226	0.245	
RMSE	0.276	0.174	.	0.233	0.283	
<b>Contest of 12 Months</b>						
True Value	0.3	0.375	.	2.0	1.0	0.0
Posterior Mean	0.307	0.341	.	2.187	1.034	
Posterior Std.	0.020	0.033	.	0.127	0.098	
RMSE	0.021	0.047	.	0.226	0.102	

Note: (1)  $MSE(\hat{\theta}) = \mathbb{E}(\hat{\theta} - \theta)^2 = [\mathbb{E}(\hat{\theta}) - \theta]^2 + Var(\hat{\theta})$  by the bias–variance decomposition. RMSE is then calculate by the squared root of MSE. (2) Players  $i$  and  $j$  submit 31 and 40 times in the 6-month contest, and 143 and 182 times in the 12-month contest, respectively.

**4.1.2. Long-Horizon Contest.** We then turn to an alternative asymptotic regime in which a single contest instance is observed over a long time horizon. Rather than increasing the number of trajectories, we examine how the accumulation of submissions over a longer period improves inference accuracy.

When generating long-horizon contest data, it is important to appropriately lower the effort costs  $c_i$  and  $c_j$  to ensure sustained effort from the contestants. This is because effort levels are influenced by the remaining time until the deadline: according to equation (7), the further away the deadline, the lower the equilibrium effort. Moreover, with volatility held constant, a long contest duration increases the likelihood that the true output gap undergoes a random walk to an unusually high level, potentially resulting in unexpected early success (Ryvkin 2022). These factors may affect the quality of the generated data.

Table 3 presents simulations of contests lasting 6 and 12 months. In the 6-month contest, we set the unit effort costs to  $c_i = 0.6$  and  $c_j = 0.75$ , resulting in 31 submissions from player  $i$  and 40 from player  $j$ . For the 12-month contest, the effort costs are reduced to  $c_i = 0.3$  and  $c_j = 0.375$ , with players  $i$  and  $j$  submitting 143 and 182 times, respectively. The posterior results show that longer contest durations and more frequent submissions lead to smaller RMSEs in the posterior distribution, indicating improved recovery of the true parameter values.

## 4.2. Out of Sample Performance

...

## 5. Empirical Application

...

### 5.1. Mapping the Model to the Real Data

To Do:

1. How to select key players?

One simple and intuitive approach is to identify the two strongest teams in each contest. This approach rests on an implicit assumption: that participants have a basic understanding of each other’s relative strength. In the context of Kaggle competitions, this is a reasonable premise: Team compositions are openly displayed, and individual profiles provide detailed historical records—such as past rankings, medal counts, and shared notebooks—which help participants quickly assess the technical strength of their rivals. Moreover, forum discussions and public notebooks foster a semi-transparent environment where ideas and methods are informally exchanged. Together, these features enable top teams to identify likely competitors and adjust their strategies accordingly.

2. How to deal with monetary prize and other forms (knowledge, reputation)? The baseline reward is “knowledge + reputation”; Later, we can verify the effect of monetary rewards (additional prize).

3. How to select contests?

## 5.2. Structural Validation

...

To Do 1: relation between  $\lambda$  and the proportion of data release?

By the data generating process (10), we have a simple maximum likelihood estimation (MLE) of the true value of  $\lambda$ . Since  $\hat{y}_t - y_t \sim \mathcal{N}(0, 1/(\lambda\Delta))$ , we have

$$\lambda^{\text{MLE}} = \frac{n}{\Delta \sum_{i=1}^n (y_i - \hat{y}_i)^2}$$

...

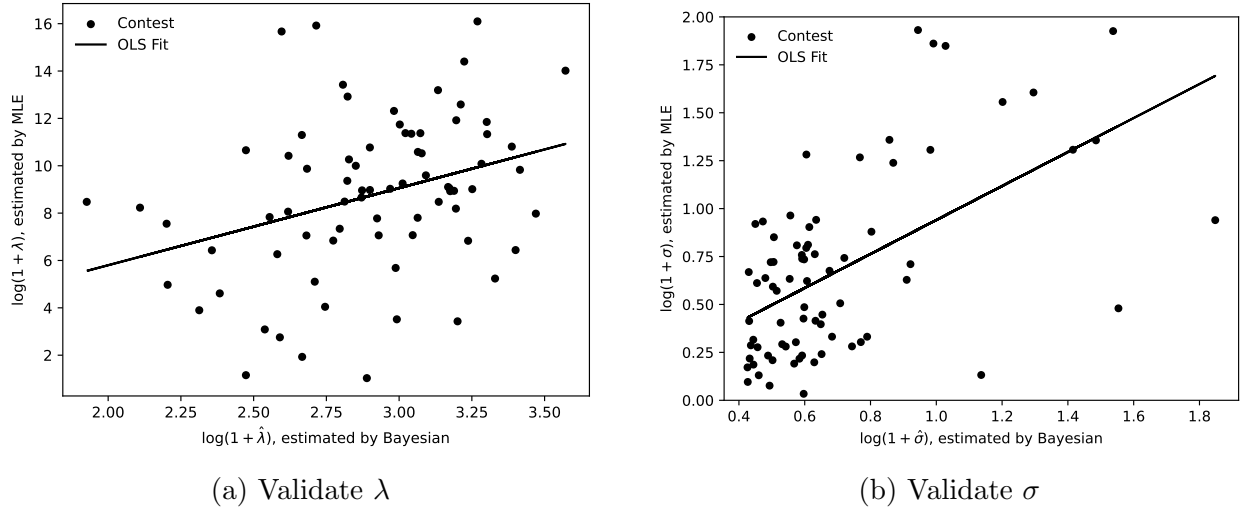


Figure 4 Structure Validation

To Do 2: validate the estimation of  $\sigma$ ?

First, we estimate submission intensities  $\tau_i(t)$  and  $\tau_j(t)$  by kernel density estimation (KDE). Having  $\hat{\tau}_i$  and  $\hat{\tau}_j$ , the effort levels of the two players are simply  $m_i(t) = \hat{\tau}_i/r$  and  $m_j(t) = \hat{\tau}_j/r$  by (8), where  $r$  is the ratio of effort level and submission intensity. Next, with the submission times denoted by  $\{t_k\}$ , we have  $y_{t_{k+1}} - y_{t_k} \sim \mathcal{N}\left(\int_{t_k}^{t_{k+1}} m_i(s) - m_j(s) ds, \sigma^2(t_{k+1} - t_k)\right)$  by the dynamic of private leaderboard (1). Then, by (21), we can estimate the parameters  $\sigma$  using MLE:

$$\sigma^{\text{MLE}} = \left( \frac{1}{n} \sum_k \frac{\left[ y_{t_{k+1}} - y_{t_k} - \int_{t_k}^{t_{k+1}} m_i(s) - m_j(s) ds \right]^2}{t_{k+1} - t_k} \right)^{1/2}$$

where  $\hat{r}$  is the Bayesian estimate.

## 6. Conclusion

...

### Appendix A: Proofs

*Proof of Lemma 2* Suppose  $\Theta = (c_i, c_j, \sigma, \lambda)$  and  $\Theta' = (c'_i, c'_j, \sigma', \lambda')$ . To show that the model parameters are jointly identifiable, it suffices to show that  $\mathcal{L}(\hat{t}_k^i, \hat{t}_k^j, \hat{y}_k | \Theta) = \mathcal{L}(\hat{t}_k^i, \hat{t}_k^j, \hat{y}_k | \Theta') \Rightarrow \Theta = \Theta'$ .  $\square$

### Appendix B: Extensions

#### B.1. Staggered Entry of Multiple Players

We index the participating teams of the contest by  $i \in \{1, 2, \dots, n\}$ . To fully leverage the potential of the data and establish a connection with our theoretical model, let's assume that each participant perceives a competitor they are playing against at every moment, denoted as  $j$ . This perceived competitor is typically understood as the most prominent individual on the leaderboard, i.e., the person ranked first. When team  $i$  themselves hold the top position, their perceived competitor is the individual who poses the greatest threat, namely the person ranked second.

#### B.2. Hybrid Kalman Filter

Let's suppose the submission events of the representative player  $i$  occur at times  $(t_1^i, t_2^i, \dots)$  following an inhomogeneous Poisson process driven by the intensity function  $\tau_i(t)$ .

After each submission, the contest designer emits a *public* signal of the real output  $x_{i,t_k}$ . The signal is ambiguous and the game holder controls the ambiguity. The dynamic of signal is

$$\hat{x}_{i,k} = x_{i,t_k} + \frac{v_{i,k}}{\sqrt{\lambda}}, \quad k = 1, 2, \dots \quad (15)$$

where  $v_{i,k}$  follows standard normal distribution and is independent with  $(W_{i,t})$  and  $(W_{j,t})$ , and the parameter  $\lambda$  is set by the game holder to control the precision of signals. The larger the  $\lambda$ , the more accurate the signal would be.

The information set of both players at time  $t \geq 0$  is  $I_t := \{\hat{x}_{i,k}, \hat{x}_{j,k} : 0 \leq t_k \leq t\}$ . Both players estimate the unknown outputs  $x_{i,t}$  and  $x_{j,t}$  purely based on the information set  $I_t$  and hidden actions  $q_{i,t}$  and  $q_{j,t}$ . Let  $\tilde{x}_{i,t} \equiv E(x_{i,t} | I_t)$  be the estimated output gap and  $S_{i,t} \equiv E[(\tilde{x}_{i,t} - x_{i,t})^2 | I_t]$  be the estimation variance. The conditional distribution  $y_t | I_t \sim \mathcal{N}(\tilde{y}_t, S_t | I_t)$  is fully captured by the mean  $\tilde{y}_t$  and variance  $S_t$ .

The evolution of  $\tilde{x}_{i,t}$  and  $S_{i,t}$  is characterized by a continuous-discrete Kalman Filter (CD-KF, [Barrau and Bonnabel 2017](#), [Frogerais et al. 2012](#)), with the measurement of each step  $k = 1, 2, \dots$  consisting of two phases: in (1) prediction phase during time interval  $(t_{k-1}, t_k)$ , equations are derived from those of Kalman-Bucy filter ([Bensoussan 1992](#)) without considering the Kalman gain:

$$d\tilde{x}_{i,t} = q_{i,t} dt \quad (16)$$

$$dS_{i,t} = \sigma^2 dt \quad (17)$$

and in (2) updation phase  $t = t_k$ , equations are

$$\tilde{x}_{i,k}^+ = \tilde{x}_{i,k}^- + \frac{\lambda S_{i,t_k}^-}{\lambda S_{i,t_k}^- + 1} (\hat{x}_{i,k} - \tilde{x}_{i,t_k}^-) \quad (18)$$

$$S_{i,t_k}^+ = \frac{S_{i,t_k}^-}{\lambda S_{i,t_k}^- + 1} \quad (19)$$

If  $\lambda = 0$ , we have  $S_t = S_0 + \sigma^2 t$ , i.e., the estimation variance is increasing in time linearly. If  $\lambda > 0$ , the estimation error decreases after each update of the public leaderboard, i.e.,  $S_{i,t_k}^+ < S_{i,t_k}^-$ .

## Appendix C: Auxiliary Results

### C.1. Solve $S_t$ in Equation (17)

If  $S$  is in steady state  $dS/dt = 0 \Leftrightarrow S = \bar{S} \equiv \sigma/\sqrt{\lambda}$ . If  $S$  is not in steady state, i.e.  $S \neq \bar{S}$ , we first isolate the two variables and get

$$\frac{dS}{\sigma - \lambda S^2} = dt$$

Then, we take the integral on both sides

$$t = \int \frac{dS}{\sigma - \lambda S^2} = \frac{1}{\sigma\sqrt{\lambda}} \int \frac{dS\sqrt{\lambda}/\sigma}{1 - (S\sqrt{\lambda}/\sigma)^2} \equiv \frac{1}{\sigma\sqrt{\lambda}} \int \frac{du}{1 - u^2}$$

where  $u = S\sqrt{\lambda}/\sigma = S/\bar{S}$ . Hence,

$$\sigma\sqrt{\lambda} \cdot t = \begin{cases} \tanh^{-1}(u) - K_1, & \text{if } |u| < 1 \\ \coth^{-1}(u) - K_2, & \text{if } |u| > 1 \end{cases} = \begin{cases} \tanh^{-1}(S/\bar{S}) - K_1, & \text{if } S < \bar{S} \\ \coth^{-1}(S/\bar{S}) - K_2, & \text{if } S > \bar{S} \end{cases}$$

Thus, we conclude the non-steady state case that

$$S = \begin{cases} \bar{S} \cdot \tanh(\sigma\sqrt{\lambda} \cdot t + K_1), & \text{if } S < \bar{S} \\ \bar{S} \cdot \coth(\sigma\sqrt{\lambda} \cdot t + K_2), & \text{if } S > \bar{S} \end{cases}$$

Finally, we determine the constants  $K_1, K_2$  by the initial condition  $S_0$  and have

$$K_1 = \tanh^{-1}(S_0/\bar{S})$$

$$K_2 = \coth^{-1}(S_0/\bar{S})$$

### C.2. MLE for $r$ and $\sigma^2$

Suppose we observe independent data points  $X_1, \dots, X_n$ , where each  $X_k \sim \mathcal{N}(M_k/r, \sigma^2 T_k)$  with known constants  $M_k$  and  $T_k$ . The goal is to estimate the parameters  $r$  and  $\sigma$  via maximum likelihood estimation (MLE). Ignoring constant terms, the log-likelihood function of the observed data is

$$\ell(r, \sigma^2) = -\frac{n}{2} \log(\sigma^2) - \frac{1}{2\sigma^2} \sum_{k=1}^n \frac{(X_k - M_k/r)^2}{T_k}.$$

To estimate  $r$ , we expand the summation of second term and have

$$Q(r) = \sum_{k=1}^n \left( \frac{X_k^2}{T_k} - \frac{2X_k M_k}{r T_k} + \frac{M_k^2}{r^2 T_k} \right) = A - \frac{2B}{r} + \frac{C}{r^2},$$

where  $A = \sum X_k^2/T_k$ ,  $B = \sum X_k M_k/T_k$ , and  $C = \sum M_k^2/T_k$ . Taking the derivative with respect to  $r$  and setting it to zero gives:

$$\frac{dQ}{dr} = \frac{2B}{r^2} - \frac{2C}{r^3} = 0 \quad \Rightarrow \quad \hat{r} = \frac{C}{B} = \frac{\sum M_k^2/T_k}{\sum X_k M_k/T_k}. \quad (20)$$

Then, substituting  $\hat{r}$  back into the likelihood, the MLE for  $\sigma^2$  is obtained by maximizing

$$\ell(\sigma^2) = -\frac{n}{2} \log(\sigma^2) - \frac{1}{2\sigma^2} \sum_{k=1}^n \frac{(X_k - M_k/\hat{r})^2}{T_k},$$

which yields

$$\hat{\sigma}^2 = \frac{1}{n} \sum_{k=1}^n \frac{(X_k - M_k/\hat{r})^2}{T_k}. \quad (21)$$



## References

- Barrau A, Bonnabel S (2017) The invariant extended kalman filter as a stable observer. *IEEE Transactions on Automatic Control* 62(4):1797–1812, ISSN 0018-9286, 1558-2523, URL <http://dx.doi.org/10.1109/TAC.2016.2594085>.
- Bensoussan A (1992) *Stochastic Control of Partially Observed Systems* (Cambridge University Press), 1 edition, ISBN 9780511526503, URL <http://dx.doi.org/10.1017/CB09780511526503>.
- Betancourt M (2017) A conceptual introduction to hamiltonian monte carlo. URL <http://dx.doi.org/10.48550/ARXIV.1701.02434>, version Number: 2.
- Bimpikis K, Ehsani S, Mostagir M (2019) Designing dynamic contests. *Operations Research* 67(2):339–356, URL <http://dx.doi.org/10.1287/opre.2018.1823>.
- Budd C, Harris C, Vickers J (1993) A model of the evolution of duopoly: Does the asymmetry between firms tend to increase or decrease? *The Review of Economic Studies* 60(3):543–573, URL <http://dx.doi.org/10.2307/2298124>.
- Frogerais P, Bellanger JJ, Senhadji L (2012) Various ways to compute the continuous-discrete extended kalman filter. *IEEE Transactions on Automatic Control* 57(4):1000–1004, ISSN 0018-9286, 1558-2523, URL <http://dx.doi.org/10.1109/TAC.2011.2168129>.
- Ghosal S, Ghosh JK, Van Der Vaart AW (2000) Convergence rates of posterior distributions. *The Annals of Statistics* 28(2), ISSN 0090-5364, URL <http://dx.doi.org/10.1214/aos/1016218228>.
- Harris C, Vickers J (1987) Racing with uncertainty. *The Review of Economic Studies* 54(1):1–21, ISSN 00346527, 1467937X, URL <http://www.jstor.org/stable/2297442>.
- Hoffman MD, Gelman A (2014) The no-u-turn sampler: Adaptively setting path lengths in hamiltonian monte carlo. *Journal of Machine Learning Research* 15(47):1593–1623, URL <http://jmlr.org/papers/v15/hoffman14a.html>.
- Lewis PAW, Shedler GS (1979) Simulation of nonhomogeneous poisson processes by thinning. *Naval Research Logistics Quarterly* 26(3):403–413, ISSN 0028-1441, 1931-9193, URL <http://dx.doi.org/10.1002/nav.3800260304>.
- Moscarini G, Smith L (2011) Optimal dynamic contests, URL [https://campuspress.yale.edu/moscarini/files/2017/01/contests\\_current-x5131k.pdf](https://campuspress.yale.edu/moscarini/files/2017/01/contests_current-x5131k.pdf), working paper.
- Neal RM (1996) *Bayesian Learning for Neural Networks*. Lecture Notes in Statistics (New York, NY: Springer New York), ISBN 978-0-387-94724-2 978-1-4612-0745-0, URL <http://dx.doi.org/10.1007/978-1-4612-0745-0>, iSSN: 0930-0325.
- Neal RM (2011) Mcmc using hamiltonian dynamics. Brooks S, Gelman A, Jones G, Meng XL, eds., *Handbook of Markov Chain Monte Carlo*, 113–162 (Chapman & Hall / CRC Press), URL <http://dx.doi.org/10.1201/b10905>, chapter 5.

- Pokern Y, Stuart A, Van Zanten J (2013) Posterior consistency via precision operators for Bayesian non-parametric drift estimation in SDEs. Stochastic Processes and their Applications 123(2):603–628, ISSN 03044149, URL <http://dx.doi.org/10.1016/j.spa.2012.08.010>.
- Ramamoorthi RV, Sriram K, Martin R (2015) On posterior concentration in misspecified models. Bayesian Analysis 10(4), ISSN 1936-0975, URL <http://dx.doi.org/10.1214/15-BA941>.
- Risdal M, Bozsolik T (2022) Meta kaggle. URL <http://dx.doi.org/10.34740/KAGGLE/DS/9>.
- Ryvkin D (2022) To fight or to give up? dynamic contests with a deadline. Management Science 68(11):8144–8165, ISSN 0025-1909, 1526-5501, URL <http://dx.doi.org/10.1287/mnsc.2021.4206>.
- Vaart AWVD (1998) Asymptotic Statistics (Cambridge University Press), 1 edition, ISBN 978-0-511-80225-6 978-0-521-49603-2 978-0-521-78450-4, URL <http://dx.doi.org/10.1017/CB09780511802256>.